

## Accepted Manuscript

The discovery and preclinical evaluation of BMS-707035, a potent HIV-1 integrase strand transfer inhibitor

B. Narasimhulu Naidu, Michael A. Walker, Margaret E. Sorenson, Yasutsugu Ueda, John D. Matiskella, Timothy P. Connolly, Ira B. Dicker, Zeyu Lin, Sagarika Bollini, Brian J. Terry, Helen Higley, Ming Zheng, Dawn D. Parker, Dedong Wu, Stephen Adams, Mark R. Krystal, Nicholas A. Meanwell

PII: S0960-894X(18)30429-3  
DOI: <https://doi.org/10.1016/j.bmcl.2018.05.027>  
Reference: BMCL 25844

To appear in: *Bioorganic & Medicinal Chemistry Letters*

Received Date: 20 February 2018  
Revised Date: 10 May 2018  
Accepted Date: 12 May 2018

Please cite this article as: Naidu, B.N., Walker, M.A., Sorenson, M.E., Ueda, Y., Matiskella, J.D., Connolly, T.P., Dicker, I.B., Lin, Z., Bollini, S., Terry, B.J., Higley, H., Zheng, M., Parker, D.D., Wu, D., Adams, S., Krystal, M.R., Meanwell, N.A., The discovery and preclinical evaluation of BMS-707035, a potent HIV-1 integrase strand transfer inhibitor, *Bioorganic & Medicinal Chemistry Letters* (2018), doi: <https://doi.org/10.1016/j.bmcl.2018.05.027>

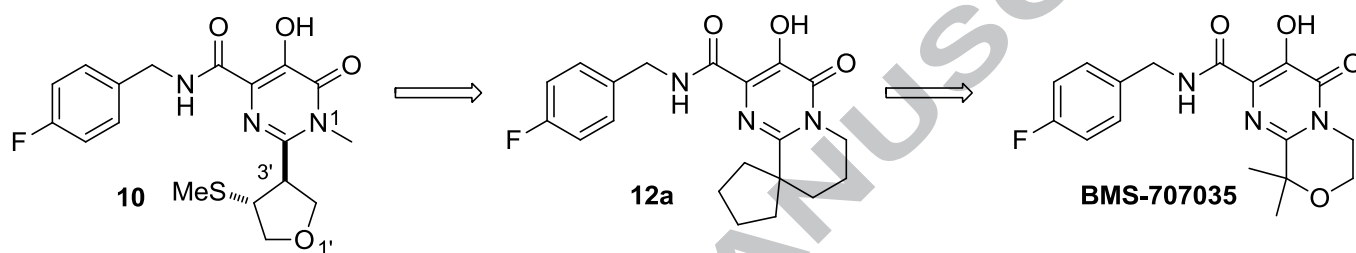
This is a PDF file of an unedited manuscript that has been accepted for publication. As a service to our customers we are providing this early version of the manuscript. The manuscript will undergo copyediting, typesetting, and review of the resulting proof before it is published in its final form. Please note that during the production process errors may be discovered which could affect the content, and all legal disclaimers that apply to the journal pertain.



## Graphical Abstract

**The discovery and preclinical evaluation of BMS-707035, a potent HIV-1 integrase strand transfer inhibitor**

B. Narasimhulu Naidu, Michael A. Walker, Margaret E. Sorenson, Yasutsugu Ueda, John D. Matiske, Timothy P. Connolly, Ira B. Dicker, Zeyu Lin, Sagarika Bollini, Brian J. Terry, Helen Higley, Ming Zheng, Dawn D. Parker, Dedong Wu, Stephen Adams, Mark R. Krystal, and Nicholas A. Meanwell



## The discovery and preclinical evaluation of BMS-707035, a potent HIV-1 integrase strand transfer inhibitor

B. Narasimhulu Naidu,<sup>1†\*</sup> Michael A. Walker<sup>1</sup>, Margaret E. Sorenson,<sup>1</sup> Yasutsugu Ueda,<sup>1</sup> John D. Matiskella,<sup>1</sup> Timothy P. Connolly<sup>1</sup>, Ira B. Dicker,<sup>2</sup> Zeyu Lin,<sup>2</sup> Sagarika Bollini,<sup>2</sup> Brian J. Terry,<sup>2</sup> Helen Higley,<sup>2</sup> Ming Zheng,<sup>3</sup> Dawn D. Parker,<sup>3</sup> Dedong Wu,<sup>4</sup> Stephen Adams,<sup>3</sup> Mark R. Krystal,<sup>2</sup> and Nicholas A. Meanwell<sup>1</sup>

<sup>1</sup>Departments of Discovery Chemistry, <sup>2</sup> Virology, <sup>3</sup>Pharmaceutical Candidate Optimization, <sup>4</sup>Materials Chemistry and Crystallography, Bristol-Myers Squibb Research and Development, 5 Research Parkway, Wallingford, Connecticut 06492.

Keywords:

HIV-1 Integrase

Strand transfer inhibitors

INSTI

Pyrimidinone carboxamides

Antiviral activity

Pharmacokinetics

**ABSTRACT:** BMS-707035 is an HIV-1 integrase strand transfer inhibitor (INSTI) discovered by systematic optimization of N-methylpyrimidinone carboxamides guided by structure-activity relationships (SARs) and the single crystal X-ray structure of compound **10**. It was rationalized that the

unexpectedly advantageous profiles of N-methylpyrimidinone carboxamides with a saturated C2-substituent may be due, in part, to the geometric relationship between the C2-substituent and the pyrimidinone core. The single crystal X-ray structure of **10** provided support for this reasoning and guided the design of a spirocyclic series **12** which led to discovery of the morpholino-fused pyrimidinone series **13**. Several carboxamides derived from this bicyclic scaffold displayed improved antiviral activity and pharmacokinetic profiles when compared with corresponding spirocyclic analogs. Based on the excellent antiviral activity, preclinical profiles and acceptable *in vitro* and *in vivo* toxicity profiles, **13a** (BMS-707035) was selected for advancement into phase I clinical trials.

---

Human immunodeficiency virus-1 (HIV-1) is the causative agent of acquired immunodeficiency syndrome (AIDS), and without treatment results in a debilitating disease that cripples the immune system of the patient, increasing susceptibility to opportunistic diseases, ultimately leading to death. Since the approval of zidovudine (AZT) as the first HIV-1 inhibitor in 1987, significant advances have been made in the treatment of HIV- infection. The current preferred treatment, referred to as highly active antiretroviral therapy (HAART) or combination antiretroviral therapy (cART), consists of combinations of two or more drugs that target specific viral processes. Since the advent of HAART, the quality of life and overall life span of the HIV-1 infected patients has significantly improved. Recent UNAIDS estimates indicate that approximately 36.7 million people are living with HIV-1 globally and that there were 1.8 million new infections and 1.0 million AIDS deaths in 2016, a significant decline when compared with the 3.4 million new infections (47%) estimated to have occurred in 2001 and 2.3 million AIDS deaths (56%) in 2005.<sup>1</sup> HIV-1 therapy requires life-long adherence to a treatment regimen that if missed can lead to the rapid development of resistance to the one or more drugs used in the combination. The development of resistance consequently limits the number of treatment options available to an infected individual. Although current drug regimens are highly efficacious and generally

well tolerated, there remain concerns about long-term toxicities. Development of cross-resistance within a mechanistic class and poor tolerability has necessitated a search for new drugs that are active against resistant viruses and safer for long-term use.

Reverse transcriptase (RT), integrase (IN) and protease (PR) are three key enzymes involved in the HIV-1 life cycle. HIV-1 integrase irreversibly inserts the nascent reverse-transcribed, double stranded viral DNA into the host genome by a multistep biochemical process.<sup>2</sup> There are two well-characterized catalytic steps involved in the integration process, the first of which is denoted as 3'-processing, in which the integrase enzyme cleaves a GT dinucleotide pair from each 3'-end of the viral cDNA long-terminal repeats, a process that occurs in the cytoplasm. The second catalytic step, referred to as strand transfer (ST), occurs in the nucleus, where integrase catalyzes the covalent insertion of reverse-transcribed, double-stranded viral DNA into the host chromosome. Inhibitors specifically targeting the inhibition of strand transfer reaction are designated as integrase strand transfer inhibitors (INSTIs).

Previously, starting from the triketoacid lead **1** (Figure 1),<sup>3</sup> optimization arrived at the amide ketoacid series **2**,<sup>4</sup> which displayed an improved antiviral activity in the cell culture HIV inhibition assay when compared with tri- or di-ketoacid derivatives. Further optimization studies focused on embedding the crucial structural elements of **2** into heterocyclic ring systems, a survey that includes pyrrolidione carboxamides **3**,<sup>5</sup> the pyrimidinone carboxamides **4**<sup>6</sup> and pyridinone carboxamides **5**. Raltegravir, the first integrase inhibitor approved for treating HIV/AIDS, belongs to the pyrimidinone class.<sup>7</sup> In this article, we describe efforts to optimize the antiviral and pharmacokinetic properties of pyrimidinone carboxamides that led to the discovery of BMS-707035 (**13a**), a candidate that was advanced into clinical trials.

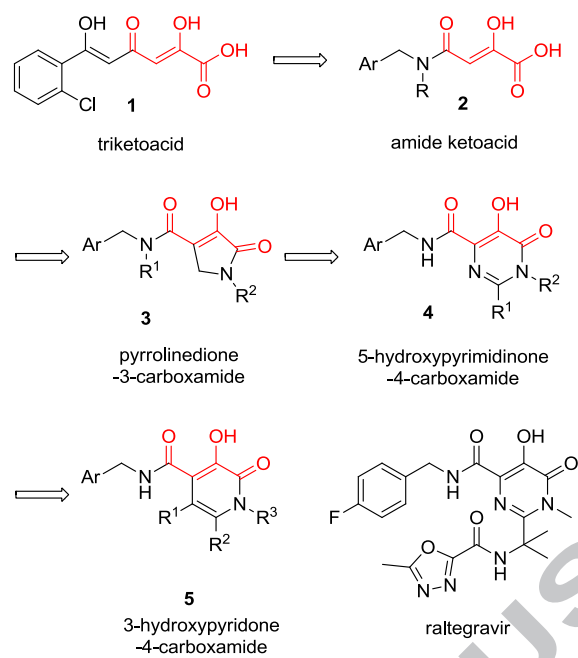
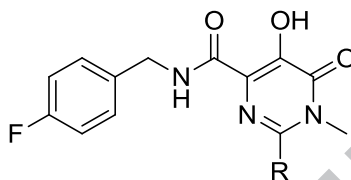


**Figure 1.** Evolution of INSTI chemotypes

Initial efforts were focused on the identification of an optimal substituent at the C2-position of the pyrimidinone core, and to this end a variety of C2-substituents were surveyed, including alkyl and cycloalkyl moieties, saturated heterocycles,<sup>8</sup> acyclic and cyclic amines,<sup>9</sup> and aryl and heteroaryl<sup>10</sup> groups. The strand transfer and cell culture inhibition data for selected compounds which form the foundation for the discovery of BMS-707035 (**13a**) are compiled in Table 1. Compounds **6–10** displayed good inhibitory activity in the strand transfer assay, which translated into potent antiviral activity in cell culture.<sup>8</sup> However, there are subtle differences in the effects of the C2-substituents based on their structural attributes. The unsaturated cyclopentenyl- and 2,5-dihydrofuranyl-substituted analogs **6** and **8** are less potent than their corresponding saturated homologues **7** and **9**, respectively. In addition, the C2-carbocyclic carboxamides **6** and **7** exhibit reduced activity in the presence of human serum albumin (HSA), attributed to their lipophilic nature, leading to a lower free fraction. Not surprisingly, the more polar C2-heterocyclic compounds **8** and **9** exhibit a more moderate loss of activity in the

presence of HSA. Remarkably, however, the C2-methylthiotetrahydrofuran carboxamide **10** not only exhibited potent cellular inhibitory activity but also displayed a lower serum shift than the tetrahydrofuran analog **9**, despite the fact that it is more lipophilic (cLogP = 0.98) than **9**, (cLogP = 0.43).

**Table 1.** Structure-activity relationships (SAR) for C2-substituted pyrimidinone carboxamide-based HIV-1 integrase inhibitor



Compd.	R	ST <sup>a</sup> IC <sub>50</sub> (nM)	EC <sub>50</sub> (nM)		Serum-shift	cLogP
			10% FBS	HSA <sup>b</sup>		
<b>6</b>		8	84	1,534	18.3	1.79
<b>7</b>		2	9	214	23.8	1.96
<b>8</b>		19	206	1,783	8.7	0.42
<b>9</b>		4	9	60	6.7	0.43
<b>10</b>		4	7	26	3.7	0.98

<sup>a</sup>ST = Strand transfer assay <sup>b</sup>HSA-EC<sub>50</sub> was determined in the presence of 10% FBS and 15 mg/mL human serum albumin

Compounds **9** and **10** were evaluated for their pharmacokinetic properties in rats and the results are summarized in Table 2.<sup>8</sup> Following intravenous (IV) administration, both compounds displayed low

clearance (CL), short half-lives ( $t_{1/2}$ ) and low volumes of distribution ( $V_{ss}$ ). When dosed orally as a solution, exposure was high and bioavailability (F) was >65% for both compounds.

**Table 2.** Pharmacokinetic profiles of **9** and **10** in male Sprague-Dawley rats

	<b>9</b>	<b>10</b>
IV dose (mg/kg) <sup>a</sup>	1	1
CL (mL/min/kg)	4.9	3.6
$t_{1/2}$ (h)	1.63	1.08
$V_{ss}$ (L/kg)	0.14	0.15
PO dose (mg/kg) <sup>a</sup>	5	5
$C_{max}$ ( $\mu$ M)	10.45	8.04
$t_{max}$ (h)	0.67	1.67
AUC ( $\mu$ M*h)	33.89	39.45
F %	68	67

<sup>a</sup>Vehicle: PEG-400/Ethanol (90:10)

It was reasoned that the subtle differences in the antiviral activity of the saturated and unsaturated matched pairs and the lower serum shift for **10** may be, in part, a function of the geometrical relationship between the pyrimidinone core and the C2-substituent. In the case of the unsaturated substituent, it was hypothesized that the  $sp^2$  hybridization of the connecting carbon would favor a coplanar arrangement between the pyrimidinone and the C2 substituent. In contrast, the tetrahedral geometry ( $sp^3$  hybridization) associated with the connecting carbon atom in the saturated analogues would theoretically favor a topography in which the pyrimidinone ring is perpendicular to the plane of the C2 substituent. In support of this hypothesis, the single crystal X-ray structure of **10** revealed the pyrimidinone core to be perpendicular to the plane of the tetrahydrofuran ring (Figure 2). With this

observation in mind, the next phase of the SAR survey focused upon designing compounds that would lock the geometric relationship between the pyrimidinone core and the C2-substituent.

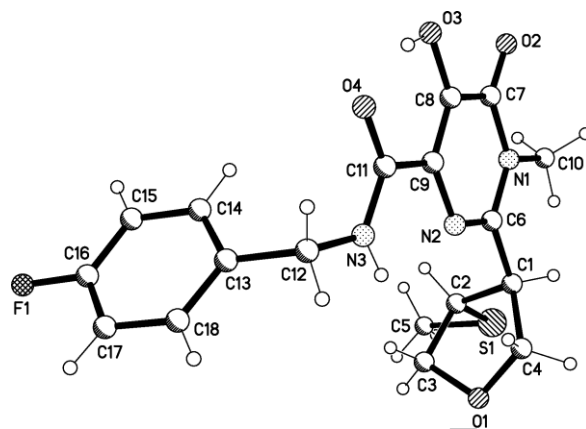


**Figure 2.** Single crystal X-ray structure of **10**.

To that end, it was envisioned that this could be accomplished by linking the pyrimidinone N1 to the 3'-carbon atom of the tetrahydrofuran ring to establish a rigid framework on which to deploy a spirocycle, as depicted conceptually by **11** in Figure 3. In this arrangement, the pyrimidinone core is perpendicular to the plane of the spirocyclic ring, thereby mimicking the topography observed in the solid state structure of **10**. This design concept was examined initially in the context of the spirocyclopentane derivative **12a** for which the single crystal X-ray confirmed the design hypothesis (Figure 4).

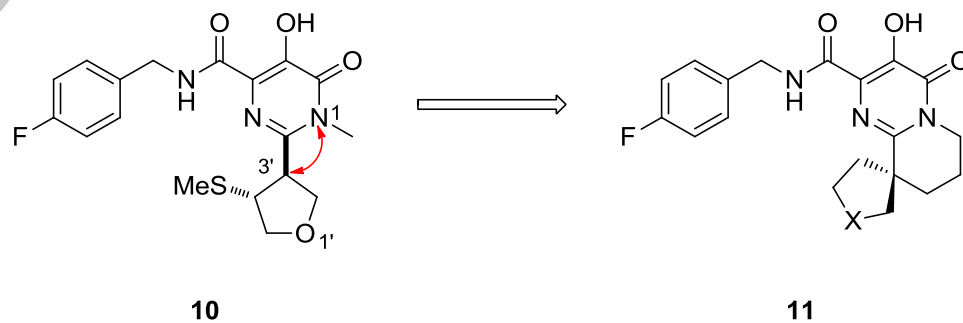


**Figure 3.** Design principle leading to the spirocyclic fused pyrimidinone chemotype **11**.

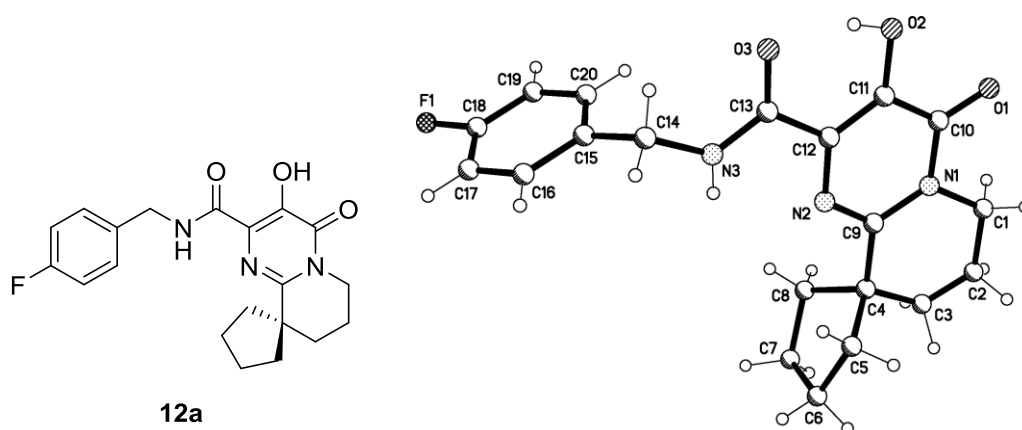
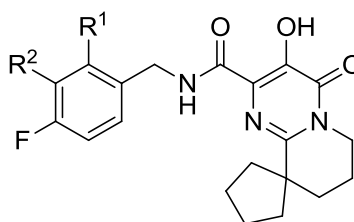


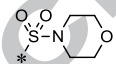
**Figure 4.** Molecular and single crystal X-ray structure **12a**

The in vitro, antiviral activity and rat clearance of the series of spirocyclic benzyl carboxamides **12a-f** are compiled in Table 3. Compound **12a** displayed superior antiviral potency compared to the progenitor **7** and, interestingly, displayed a lower serum shift despite being more lipophilic than **7**. Benzylamide **12b**, containing a lipophilic *ortho*-methyl substituent, maintained both the intrinsic enzyme inhibition and antiviral activity of **12a**, but suffered from a substantial (30-fold) loss of activity in the presence of HSA. In an effort to reduce the effect of serum, the benzylamides series **12c-f** incorporating hydrophilic substituents were surveyed. The methylsulfonyl-substituted analog **12c** displayed potent antiviral activity with a modest 8-fold shift in the  $EC_{50}$  value in the presence of HSA, whereas the dimethylsulfamoyl analog **12d** exhibited slightly reduced activity in both the strand transfer and cell culture inhibition assays compared to **12a** with or without added human serum albumen. On the other hand, the morpholinosulfonamide analog **12e** exhibited reduced potency in the biochemical assay but demonstrated a similar antiviral profile to **12a** in both cell culture assays. Lastly, the cyclic sulfonamide **12f** exhibited a comparable antiviral profile to **12a** in all three assays. Of the spirocyclic

carboxamide derivatives that were evaluated in a rat IV pharmacokinetic screen, **12a** and **12b** displayed intermediate clearance values, while **12c** exhibited high clearance.

**Table 3.** Structure activity relationships for spirocycle pyrimidinone carboxamides **12a-f**



Compd.	R <sup>1</sup>	R <sup>2</sup>	ST IC <sub>50</sub> <sup>a</sup> (nM)	EC <sub>50</sub> (nM)		cLogP	Rat CL <sup>c</sup> (mL/min/kg)
				10% FBS	HSA <sup>b</sup>		
<b>12a</b>	H	H	3	2	19	2.49	18
<b>12b</b>	H	Me	2	5	149	3.00	17
<b>12c</b>	S(O) <sub>2</sub> Me	H	4	1	8	1.30	46
<b>12d</b>	S(O) <sub>2</sub> NMe <sub>2</sub>	H	6	3	27	1.49	nd <sup>d</sup>
<b>12e</b>		H	11	3	14	1.30	nd
<b>12f</b>		H	5	2	21	1.55	nd

<sup>a</sup>ST = Strand transfer, <sup>b</sup>HSA-EC<sub>50</sub> values were determined in the presence of 10% FBS and 15 mg/mL human serum albumin, <sup>c</sup>Male Sprague-Dawley rats were administered a 1 mpk IV dose of the compound in a vehicle of PEG400/Ethanol (90:10) and blood samples were collected at 5 and 30 min and 1, 2 and 4 h following drug administration. <sup>d</sup>nd = not done

Although the spirocyclic derivatives **12a-f** demonstrated targeted antiviral potency, these compounds still suffered from poor pharmacokinetic and pharmaceutical/physicochemical properties. These compounds displayed aqueous solubility of less  $\leq 5$   $\mu\text{g/ml}$ , providing a focus for further optimization that was also anticipated to offer the potential for enhanced pharmacokinetic properties. To reduce the lipophilicity of **12a**, the effect of replacing the cyclopentyl ring with a gem-dimethyl moiety was explored, while the introduction of a heteroatom into the fused B ring was examined as an avenue toward further increasing polarity (Figure 5). The initial efforts were directed at scaffold **13a** which incorporates an embedded morpholine heterocycle, a moiety that has found extensive application as a means of improving physicochemical properties. Analysis of developability data for compounds containing a variety of heterocyclic rings has found that those containing a morpholine heterocycle fared well when compared to other heterocycles, generally displaying improved aqueous solubility, lower protein binding and a lower potential for CYP450 inhibition.<sup>11</sup> This scaffold was anticipated to exhibit reduced lipophilic character as reflected in the LogP value of 1.02 calculated for **13a** which is substantially lower than the LogP of 2.49 calculated for **12a**.

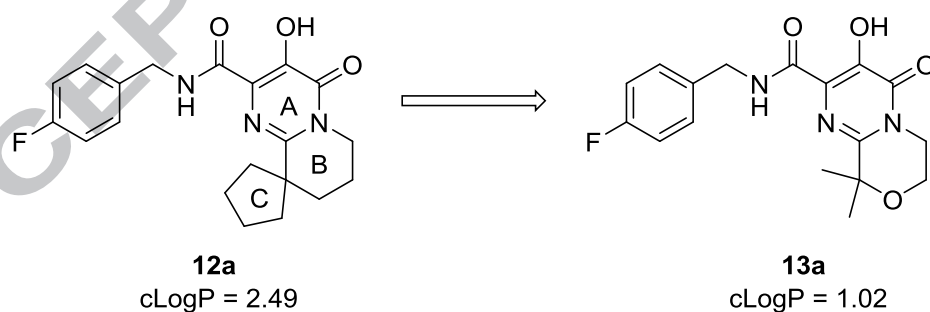
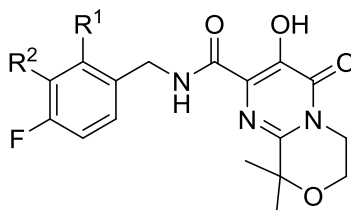


**Figure 5.** Design of morpholine embedded pyrimidinone scaffold

The biochemical, cell culture activities and in vivo properties of bicyclic carboxamides **13a-j** are compiled in Table 4, with the prototype of the series, 4-fluorobenzyl carboxamide **13a**, displaying an antiviral profile comparable to the spirocyclic carboxamide **12a**. The introduction of a small hydrophobic methyl (**13b**) and chloride (**13c**) substituents at the *meta*-position of the benzyl ring did not significantly affect the intrinsic antiviral activity, although the HSA-derived potency shift was exacerbated. In contrast, in the presence of HSA, the *ortho*-methyl and *ortho*-chloro analogs **13d** and **13e**, respectively, exhibited substantially reduced activities. In contrast to the observations made with **13d-e**, analogs **13f-j**, containing polar *ortho*-substituents, exhibited potent antiviral activities and displayed lower potency shift in the presence of HSA. The morpholino analog **13f** showed potent antiviral activity that was reduced about 10-fold in the presence of HSA. The *ortho*-methylcarboxamide **13g** displayed an interesting profile, expressing potent antiviral activity that was negligibly affected by HSA in spite of reduced potency in the biochemical assay. Finally, the methylsulfonyl (**13h**), the dimethylsulfamoyl (**13i**) and the cyclic-sulfonamide (**13j**) analogs exhibited potent antiviral activities that were subject to modest  $\leq 4$ -fold shift in the EC<sub>50</sub> value in the presence of HSA. Several of these compounds were evaluated in rat pharmacokinetic studies and the clearance data following IV dosing is presented in the Table 4. Compounds **13a**, **13b** and **13h** displayed low clearance whereas **13f**, **13g**, **13i** and **13j** exhibited moderate to high clearance in the rat.

**Table 4.** Enzyme inhibitory and antiviral data for pyrimidinone carboxamides **13a-j**



Compd.	R <sup>1</sup>	R <sup>2</sup>	ST IC <sub>50</sub> <sup>a</sup> (nM)	EC <sub>50</sub> (nM)		cLogP	Rat CL <sup>c</sup> (mL/min/kg)
				10% FBS	HSA <sup>b</sup>		

<b>13a</b>	H	H	3	2	17	1.02	9.6
<b>13b</b>	H	Me	3	1	90	1.53	11
<b>13c</b>	H	Cl	3	2	84	1.63	nd <sup>d</sup>
<b>13d</b>	Me	H	2	21	557	1.53	nd
<b>13e</b>	Cl	H	10	53	857	1.63	nd
<b>13f</b>		H	5	2	19	0.90	29
<b>13g</b>	CO <sub>2</sub> NHMe	H	11	2	3	0.09	22
<b>13h</b>	S(O) <sub>2</sub> Me	H	6	3	6	-0.17	6.9
<b>13i</b>	S(O) <sub>2</sub> NMe <sub>2</sub>	F	10	3	12	0.02	62
<b>13j</b>		H	9	2	7	0.08	38

<sup>a</sup>ST = Strand transfer, <sup>b</sup>HSA-EC<sub>50</sub> were determined in the presence of 10% FBS and 15 mg/mL human serum albumin, <sup>c</sup>Male Sprague-Dawley rats were administered a 1 mpk IV dose of the compound in a vehicle of PEG400/Ethanol (90:10) and blood samples were collected at 5 and 30 min and 1, 2 and 4 h following drug administration. <sup>d</sup>nd = not done.

Compound **13a** with potent antiviral activity and low potency-shift ( $\leq 10x$ ) in the presence of either 15 mg/mL HSA or 40% human serum (HS) was further evaluated in additional *in vitro* studies, the results of which are summarized in Table 5. Plasma protein binding of **13a** was high in all species ( $\geq 93.7\%$ ) and the compound was not overtly cytotoxic to several cell lines, with CC<sub>50</sub> values of  $\geq 45 \mu\text{M}$ . The crystalline solubility of **13a** ranged from 9 to 63  $\mu\text{g/mL}$  in the physiological pH range at room

temperature and increased as the pH increased, all the while demonstrating satisfactory solution and solid-state stability under various conditions. Caco-2 studies revealed high permeability with no indication of efflux. In studies designed to assess the potential for drug-drug interactions, the IC<sub>50</sub> values toward human CYP1A2, CYP2C9, CYP2C19, CYP2D6 and CYP3A4 enzymes were >40 μM, classifying **13a** as a relatively weak CYP inhibitor, for which drug interactions involving CYP substrates were not anticipated. Minimal transactivation of human PXR (EC<sub>20A</sub> and EC<sub>60A</sub> > 50 μM) or induction of CYP3A4 mRNA (tested up to 100 μM of **13a** in Fa2N-4 immortalized human hepatocytes) was observed, and thus, significant induction of CYP3A4 was not expected. Compound **13a** was not a substrate of human P-glycoprotein (P-gp) and was a relatively weak inhibitor of this efflux pump (5% inhibition of [<sup>3</sup>H]-digoxin transport at 10 μM), and, therefore, drug interactions involving P-gp were not expected. The half-life values of **13a** in a phase I metabolic oxidation assay (CYP-NADPH) were ≥ 96 minutes in human, dog, monkey and rat, data that suggest low potential for oxidation by the CYPs. Compound **13a** was not mutagenic in a bacterial reverse mutation assay (*Salmonella typhimurium* strains TA98 and TA100) at ≤5000 μg/plate with and without metabolic activation. An *in vitro* cytokinesis-blocked micronucleus study was performed to determine the potential of **13a** to induce micronuclei in cultured Chinese hamster ovary (CHO) cells exposed to ≤500 μg/mL **13a** (≈1.4 mM). Compound **13a** was not clastogenic in CHO cells exposed either to ≤1.4 mM for 3 hours in the presence of metabolic activation or to ≤0.36 mM for 22.5 hours in the absence of metabolic activation.

**Table 5.** *In vitro* profiling data for **13a**.

---

Molecular weight	347.34
------------------	--------

---

ST-IC <sub>50</sub>	3 (n = 98) nM
10% FBS-EC <sub>50</sub>	2.5 (n = 23) nM
15 mg/mL HSA-EC <sub>50</sub>	16.5 (n = 14) nM
40% HS-EC <sub>50</sub>	25.2 (n = 18) nM
Plasma protein binding	93.7% (rat), 95.9% (cyno), 98.5% (dog), 97.6% (human)
CC <sub>50</sub>	>200 (n = 44) μM
HEPG2-Cytotoxicity IC <sub>50</sub>	≥45 μM
Physicochemical properties	Melting point = 179-180 °C Experimental Log <i>D</i> = 2.02 at pH 6.5 Experimental p <i>K</i> <sub>a</sub> = 6.6 ± 0.2 cLogP = 1.02
Solubility	9 μg/mL at pH 2.3, 21 μg/mL at pH 6.1 63 μg/mL at pH 7.3 and 234 μg/mL at pH 8.5
Caco-2, (3 μM) AB/BA	334/240 nm/sec
CYP inhibition IC <sub>50</sub>	All >40 μM
PXR-TA EC <sub>50</sub>	>50 μM
CYP-NADPH t <sub>1/2</sub>	>120 (rat), 96 (cyno), 107 (dog), 110 (human) min
Genotoxicity	Ames TA98: negative <i>In vitro</i> micronucleus: negative

---

Compound **13a** emerged as a lead compound based on its antiviral activity and *in vitro* lead profiling properties and was advanced into full pharmacokinetic profiling studies in three preclinical species. The results of pharmacokinetic studies conducted in the rat, monkey, and dog, performed using PEG 400/ethanol (90:10) solutions, are summarized in Table 5. Compound **13a** was characterized as a low clearance compound in the rat, dog and monkey with moderate to long elimination half-lives in all species. The volume of distribution was low across the species, indicating that compound distribution outside of the plasma is minimal. When **13a** was dosed in solution, the oral exposure was high and absolute oral bioavailabilities ranged between 56 and 129%. The  $t_{\max}$  of 0.25 h suggests rapid absorption of the compound in all 3 species. In dog cardiovascular and two week rat toxicity studies, **13a** (BMS-707035) demonstrated good safety margins data that collectively contributed to its selection as a clinical candidate

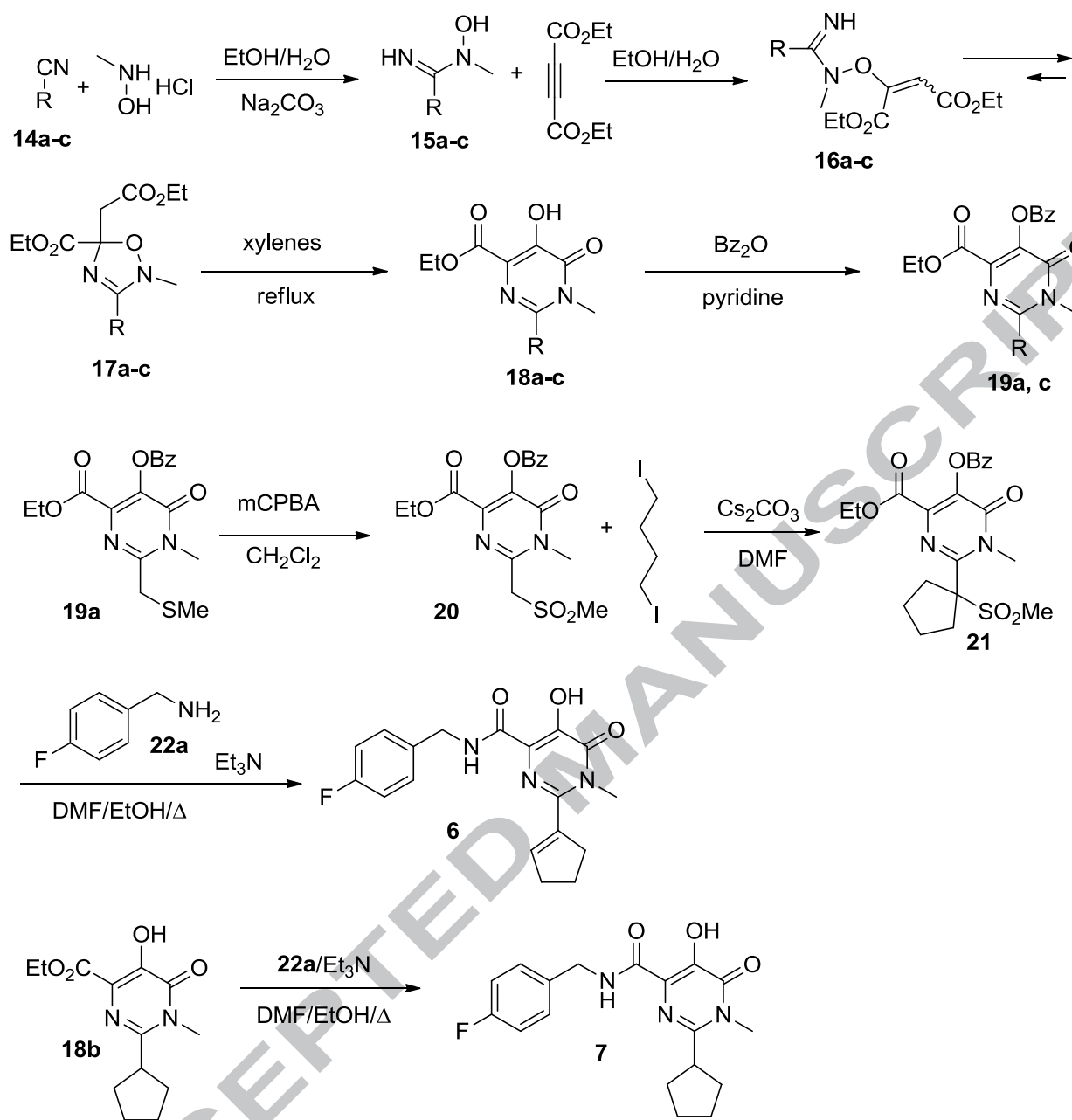
**Table 5.** Pharmacokinetic profiling data for **13a** in the rat, monkey and dog

	Rat <sup>a</sup>	Monkey <sup>b</sup>	Dog <sup>c</sup>
IV dose (mg/kg) <sup>d</sup>	0.87	1	1
CL (ml/min/kg)	9.7	6.8	2.0
$t_{1/2}$ (h)	4.0	6.5	6.0
$V_{ss}$ (L/kg)	0.86	0.87	0.45
PO dose (mg/kg) <sup>d</sup>	4.4	5	5.2
$C_{\max}$ ( $\mu$ M)	4.51	6.12	72.8
$t_{\max}$ (h)	0.25	0.25	0.25
AUC ( $\mu$ M*h)	19.1	19.2	162
F %	86	56	129

<sup>a</sup>Male Sprague-Dawley rats, <sup>b</sup>cynomolgus monkeys, <sup>c</sup>beagle dogs, <sup>d</sup>Vehicle: PEG-400/Ethanol (90/10, v/v) solution

The synthesis of C2-substituted pyrimidinone carboxamides **6-10** is outlined in Schemes 1 and 2. Treatment of readily accessible nitriles **14a-c** with N-methylhydroxylamine hydrochloride in the presence of base provided the adducts **15a-c**, which were subsequently reacted with diethyl acetylenedicarboxylate to afford inseparable mixtures of **16a** and **17a** with nitrile **14a** or 2,5-dihydro-1,2,4-oxadiazole intermediates **17b-c** with nitriles **14b-c**.<sup>12</sup> Heating a xylenes solution of **16a** or **17a-c** at reflux provided the desired pyrimidinone esters **18a-c**.<sup>13</sup> Treatment of **18a** and **18c** with benzoic anhydride in pyridine furnished benzoate esters **19a** and **19c**. Oxidation of intermediate **19a** with mCPBA yielded the sulfone **20**, which was subsequently converted into cyclopentyl derivative **21** by reacting with 1,4-diiodobutane in the presence of Cs<sub>2</sub>CO<sub>3</sub>. Finally, heating **21** with 4-fluorobenzylamine and triethylamine provided the final compound **6**, the methylsulfonyl moiety was expelled by retro-ene reaction under thermal condition. The C2-cyclopentyl compound **7** was prepared by heating intermediate **18b** with 4-fluorobenzylamine.

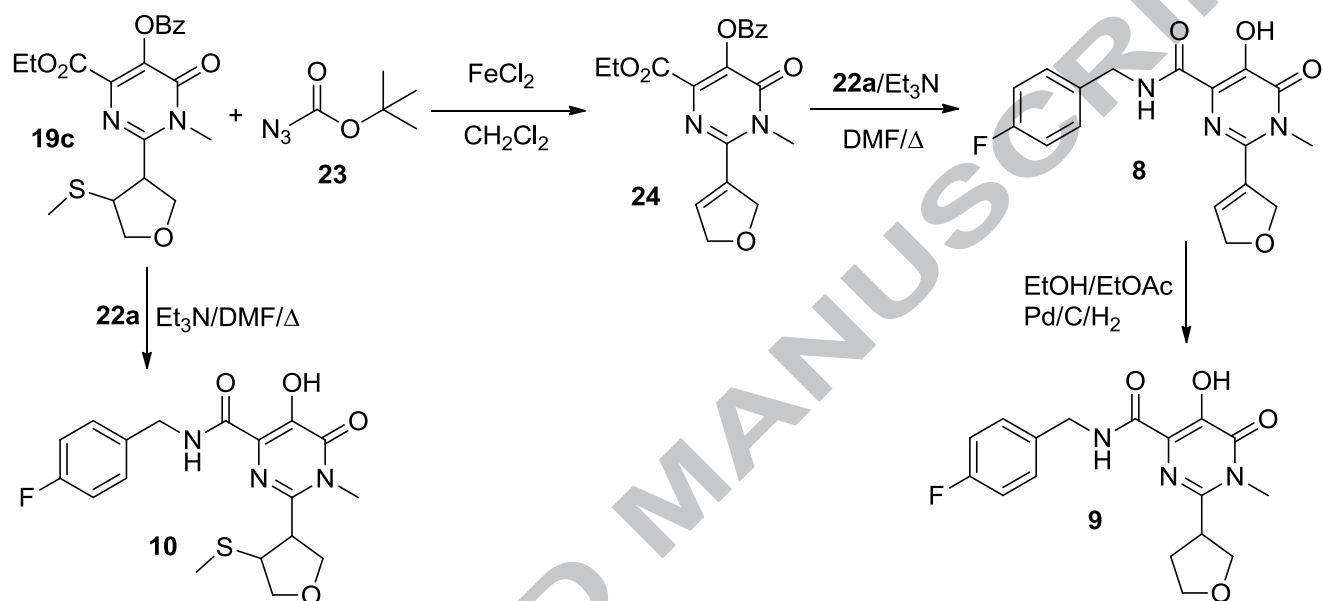
**Scheme 1.** Synthesis of **6** and **7**



Treatment of methylthiofuranyl intermediate **19c** with *tert*-butyl carbonazide (Boc-N<sub>3</sub>) in the presence of anhydrous ferrous chloride furnished the 2,5-dihydrofuranyl derivative **24**. Reaction of Boc-N<sub>3</sub> with **19c** generates a transient sulfanylidene intermediate which instantaneously undergoes retro-ene reaction to afford **24**. Heating **24** with 4-fluorobenzylamine and triethylamine yielded final compound **8**, which was subsequently converted to C2-tetrahydrofuran-3-yl derivative **9** by reducing the

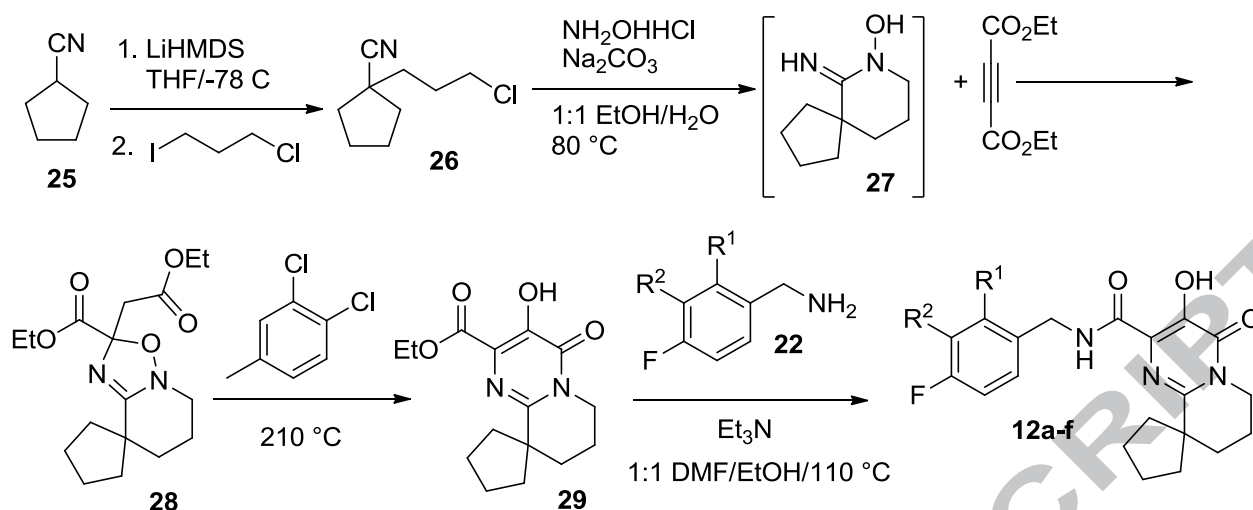
double bond under hydrogenation condition. Methylthiotetrahydrofuran analog **10** was obtained by heating **19c** with excess 4-fluorobenzylamine and triethylamine in DMF.

**Scheme 2.** Synthesis of **9** and **10**



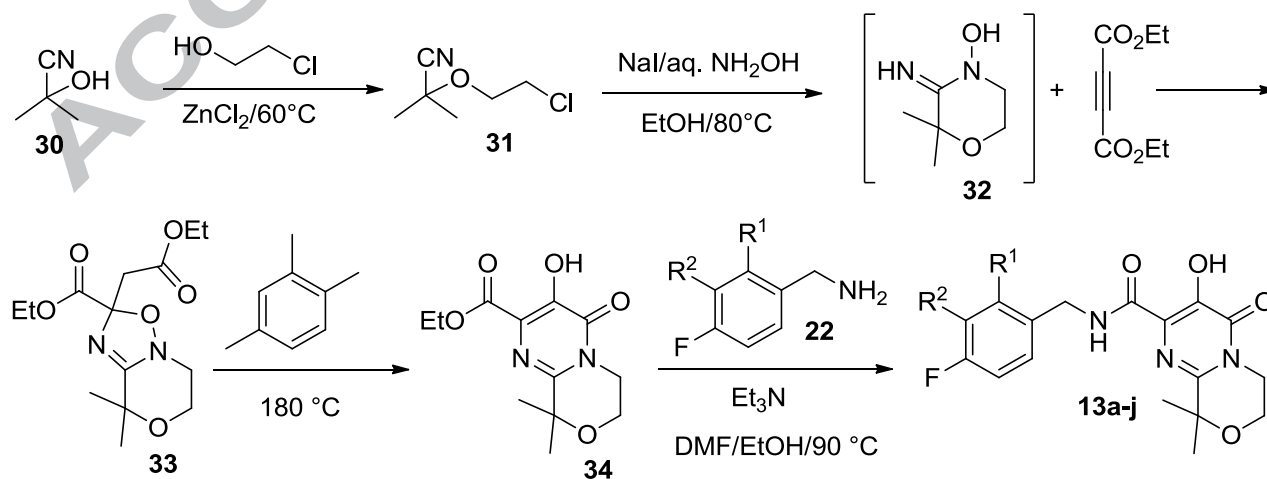
The spirocyclic pyrimidinone carboxamides **12a-f** were prepared following the synthesis sequence shown in Scheme 3. Alkylation of cyclopentylcarbonitrile **25** with 3-chloro-4-iodopropane led to the intermediate **26**. Heating **26** with hydroxylamine hydrochloride in the presence of base gave spirocyclic intermediate **13**, which when treated with diethyl acetylenedicarboxylate yielded the tricyclic spirocycle **28**. Upon heating the solution of **28** in refluxing 2,4-dichlorotoluene afforded the desired pyrimidinone ester **29**. The final spirocyclic pyrimidinone carboxamides **12a-f** were prepared by heating **29** with appropriate benzylamine **22** in the presence of triethylamine.

**Scheme 3.** Synthesis of spirocyclic pyrimidinone carboxamides **12**



Finally, the bicyclic pyrimidinone carboxamides **13a-j** were prepared in five steps starting from simple starting materials as illustrated in Scheme 4. The nitrile **31** was prepared from acetone cyanohydrin and 2-chloroethanol by following the procedure reported in the literature.<sup>14</sup> Treatment of **31** with 50% aqueous hydroxylamine in the presence of sodium iodide provided intermediate **32**, which upon exposure to diethyl acetylenedicarboxylate yielded intermediate **33**. Pyrolysis of **33** in boiling 1,2,4-trimethylbenzene furnished the pyrimidinone ester **34**, which was converted into the desired carboxamides **13a-j**<sup>15</sup> by reacting **34** with appropriate benzylamine **22** and triethylamine at 90 °C.

#### Scheme 4. Synthesis of pyrimidinone carboxamides **13**



Observations of differences in the biological activities between the unsaturated and saturated C2-substituted pyrimidinone carboxamides led to the hypothesis that the geometric arrangement between the C2-substituent and the pyrimidinone core was an important factor. This led to the concept of a spirocycle-based pyrimidinone chemotype designed to mimic what was hypothesized to be the bound conformation of **10**. The synthesis and evaluation of the spirocyclic carboxamides **12a-f** validated the design proposal, but these molecules suffered from poor physicochemical and pharmacokinetic properties. This was addressed by truncating the spirocyclic ring and introducing a heteroatom into the fused saturated ring of **12** to provide compounds with reduced lipophilicity. The antiviral activity, preclinical pharmacokinetics and safety profile of BMS-707035 (**13a**) supported continued development into phase I clinical trials conducted in normal healthy human volunteers. Single oral doses of 200, 600, 800 and 1200 mg of **13a** were well tolerated with no clinically significant adverse events noted. The mean  $C_{24h}$  following the 600 mg QD dose was 340 ng/mL which is approximately 1.9-fold the protein binding-adjusted- $EC_{90}$  value of 180 ng/mL, lending support to a 600 mg QD dose being sufficient to significantly inhibit viral replication in HIV-1-infected subjects. Unfortunately, further development of **13a** was halted due to the occurrence of convulsions in two dogs with high  $C_{max}$  exposure ( $\geq 67$   $\mu\text{g/mL}$ ) in a 12 month toxicological study.

### Corresponding Author

\*B. Narasimhulu Naidu, Email: [b.n.naidu@viihealthcare.com](mailto:b.n.naidu@viihealthcare.com). Phone: +1-203-643-6455

### Present Address

<sup>†</sup>ViiV Healthcare, 36 East Industrial Road, Branford, CT 06405, USA.

## ACKNOWLEDGMENTS

The authors would like to thank members of the Department of Discovery Synthesis (DDS) and Biocon-Bristol Myers Squibb Research Center (BBRC) for scaling up key intermediates, analytical team for analytical experiments, lead profiling group for evaluating compounds in an *in vitro* ADME&T assays and discovery toxicology team for *in vivo* safety assessment in dogs and rats.

## REFERENCES

1. <http://www.unaids.org/en/resources/fact-sheet>; accessed Sept 1, 2017. .
2. Craigie, R. The molecular biology of HIV integrase. *Future Virol.* 2012;7:679-686
3. Reference for compound 1; a) Sechi, M.; Sannia, L.; Carta, F.; Palomba, M.; Dallochio, R.; Dessi, A.; Derudas, M.; Zawahir, Z. Neamati, N. Design of novel bioisostere of beta-diketo acid inhibitors of HIV-1 integrase. *Antivir. Chem. Chemother.* 2005;16:41-61. B) Walker, M. A.; Johnson, T.; Ma, Z.; Banville, J.; Remillard, R.; Kim, O.; Zhang, Y.; Staab, A.; Wong, H.; Torri, A.; Samanta, H.; Lin, Z.; Deminie, C.; Terry, B.; Krystal, M. Meanwell, N. Triketoacid inhibitors of HIV-integrase: A new chemotype useful for probing the integrase pharmacophore. *Bioorg. Med. Chem. Lett.* 2006;16:2920-2924.
4. (a) Walker MA, Banville J, Johnson T, Ma Z, Remillard R, Plamondron S, Bouthillier G, Martel A, Torri AF, Casperson M, Bollini S, Terry BJ, Lin Z, Samanta HK, Krystal M, Zheng M, Meanwell NA. 2009. Optimization of compound efficiency in the context of discovering an amide ketoacid based HIV-integrase inhibitor with oral antiviral activity. 237<sup>th</sup> ACS National Meeting, Salt Lake City, UT, USA, March 22-26, 2009, poster # MEDI 204. (b) Walker, M. A.; Johnson, T.; Ma, Z.; Zhang, Y.; Banville, J.; Remillard, R.; Plamondon, S.; Pendri, A.; Wong,

- H.; Smith, D.; Torri, A.; Samanta, H.; Lin, Z.; Deminie, C.; Terry, B.; Krystal, M. Meanwell, N. Exploration of the diketoacid integrase inhibitor chemotype leading to the discovery of the anilide-ketoacids chemotype. *Bioorg. Med. Chem. Lett.* 2006;16:5818-5821.
5. Naidu, B. N.; Banville, J.; Bollini, S.; Bouthillier, G.; Gulgeze, H. G.; Johnson, T.; Krystal, M.; Lin, Z.; Martel, A.; Meanwell, N. A.; Parker, D. D.; Plamondon, S.; Remillard, R.; Samanta, H. K.; Sorenson, M. S.; Terry, B. J.; Torri, A. F.; Walker, M. A.; Zhenh, M.; Zupping, M. Design, synthesis and HIV-1 integrase inhibitory activity of N-benzyl-4-hydroxy-5-oxo-2,5-dihydro-1H-pyrrole-3-carboxamides. The 237<sup>th</sup> American Chemical Society National Meeting, Salt Lake City, UT, March 22-26, 2009, poster # MEDI 205.
6. Three groups independently discovered pyrimidinone carboxamides as INSTIs: (a) Di Francesco, M. E.; Gardelli, C.; Harper, S.; Matassa, V. G.; Muraglia, E.; Nizi, E.; Pace, P.; Pacini, B.; Petrocchi, A.; Pioma, M.; Summa, V. Dihydroxypyrimidine carboxamide inhibitors of HIV integrase. World Patent Application WO 2003035076, May 1<sup>st</sup>, 2003.; (b) Walker, M.; Gulgeze, H. B.; Naidu, B. N.; Sorenson, M. E.; Ueda, Y.; Matiskella, J. HIV integrase inhibitors. World Patent Application WO 2004062613, July 29<sup>th</sup>, 2004.; (c) Fuji, M.; Matsushita, S.; Mikamiyama, H. Antiviral agents containing nitrogen-containing heteroaromatic compounds. Japan Kokai Tokyo Koho JP 2004244320, September 2<sup>nd</sup>, 2004.
7. Summa, V.; Petrocchi, A.; Bonelli, F.; Crescenzi, B.; Donghi, M.; Ferrara, M.; Fiore, F.; Gardelli, C.; Paz, O. G.; Hazuda, D. J.; Jones, P.; Kinzel, O.; Laufer, R.; Monteaguda, E.; Muraglia, E.; Nizi, E.; Orvieto, F.; Pace, P.; Pescatore, G.; Scarpelli, R.; Stillmock, K.; Witmer, M. V.; Rowley, M. Discovery of Raltegravir, a potent, selective orally bioavailable HIV-integrase inhibitor for the treatment of HIV-AIDS infection. *J. Med. Chem.* 2008;51:5843-5855.

8. (a) Naidu, B.N.; Sorenson, M. E.; Patel, M.; Ueda, Y.; Banville, J.; Beaulieu, F.; Bollini, S.; Dicker, I.; Higley, H.; Lin, Z.; Pajor, L.; D. Parker, D.D; Terry, B.; Zheng, M.; Martel, A.; Meanwell, N. A.; Krystal, M.; Walker, M. A. The Synthesis and HIV-1 Integrase Inhibitory Activity of C2-C-Linked Heterocyclic-5-hydroxy-6-oxo-dihydropyrimidine-4-carboxamides. The 240<sup>th</sup> American Chemical Society National Meeting, Boston, MA, March 22-26, 2009, poster # MEDI 130. (b) Naidu, B.N.; Sorenson, M. E.; Patel, M.; Ueda, Y.; Banville, J.; Beaulieu, F.; Bollini, S.; Dicker, I.; Higley, H.; Lin, Z.; Pajor, L.; D. Parker, D.D; Terry, B.; Zheng, M.; Martel, A.; Meanwell, N. A.; Krystal, M.; Walker, M. A. The Synthesis and evaluation of C2-carbon-linked heterocyclic-5-hydroxy-6-oxo-dihydropyrimidine-4-carboxamides as HIV-1 Integrase Inhibitors. *Bioorg. Med. Chem. Lett.* 2015;25:717-720.
9. Sorenson, M.; Naidu, B. N.; Matiskella, J.; Connolly, T.; Ueda, Y.; Meanwell, N. A.; Bollini, S.; Samanta, H. K.; Terry, B. J.; Lin, Z.; Dicker, I.; Parker, D.; Pajor, L.; Zheng, M; Krystal, M.; Walker, M. A. Study of C 2-N-linked heterocyclic pyrimidin-6-oxa-5-hydroxy-4-carboxamide derivatives as HIV integrase inhibitors. The 240<sup>th</sup> American Chemical Society National Meeting, Boston, MA, March 22-26, 2009, poster # MEDI 133.
10. Sorenson, M.; Bollini, S.; Casperson, M.; Krystal, M.; Lin, Z.; Meanwell, N.; Naidu, B. N.; Samanta, H.; Terry, B.; Torri, A.; Walker, M. 2-Aryl substituted pyrimidin-6-oxa-5-hydroxy-4-carboxamides as HIV integrase inhibitors. The 36<sup>th</sup> ACS Northeast Regional Meeting 2009, Hartford, CT, October 7-10, 2009, poster # 74284.
11. Ritchie, T. J.; Macdonald, S. J. F.; Peace, S.; Pickett, S. D.; Luscombe, C. N. The developability of heteroaromatic and heteroaliphatic rings-do some have a better pedigree as potential drug molecules than others? *Med. Chem Commun.* 2012;3:1062-1069.

12. Naidu, B. N.; Sorenson, M. E. Facile One-pot synthesis of 2,3,5-substituted-1,2,4-oxadiazolines from nitriles in aqueous solution. *Org. Lett.* 2005;7:1391-1393.
13. Naidu, B. N. Tandem retro-Michael addition/Claisen rearrangement/intramolecular cyclization: One-pot synthesis of densely functionalized ethyl dihydropyrimidine-4-carboxylates from simple building blocks. *Synlett*, 2008;547-550. b) Pye, P. J.; Zhong, Y. L.; Jones, G. O.; Reamer, R. A.; Houk, K. N.; Askin, D. A polar radical pathway to assemble the pyrimidinone core of HIV integrase inhibitor raltegravir potassium. *Angew. Chem. Int. Ed.* 2008;47:4134-4136.
14. a) Navalokina, R. A.; Zil'berman, E. N. Production of unsymmetrical ethers from 2-hydroxyisobutyronitrile and various alcohols. *J. Org. Chem. USSR (Engl. Trans.)*, 1980;16:1382-1386. b) Ramalingam, K. Process for preparing 2-methoxyisobutylisonitrile. United States Patent US 4864051, September 5<sup>th</sup>, 1989.
15. Compound **13a**: To a solution of ethyl 3-hydroxy-9,9-dimethyl-4-oxo-4,6,7,9-tetrahydropyrimido[2,1-c][1,4]oxazine-2-carboxylate, (3.0 g, 11.19 mmol) in DMF (20 mL) and ethanol (10 mL) was added triethylamine (1.55 mL) followed by 4-fluorobenzylamine (3.82 mL, 33.57 mmol). The mixture was stirred at 90 °C for 2 h and then concentrated. The resultant oil was partitioned between ethyl acetate (50 mL) and 1N aqueous HCl (35 mL). The aqueous layer was back-extracted with ethyl acetate (20 mL) and the organic layers were combined and washed with H<sub>2</sub>O (4 x 20 mL) and brine then dried (Na<sub>2</sub>SO<sub>4</sub>) and concentrated. The brown residue was triturated with ether and the solids filtered and washed with ether. The pale brown solids were recrystallized from 95:5 MeOH/H<sub>2</sub>O to give the title compound as a colorless needles (3.18 g, 82% yield). <sup>1</sup>H NMR (500 MHz, CDCl<sub>3</sub>) δ: 11.96 (1H, s), 7.77 (1H, brs), 7.30 (2H, dd, *J* = 8.4, 5.3 Hz), 7.04 (2H, t, *J* = 8.7 Hz), 4.57 (2H, d, *J* = 6.1 Hz), 4.01 (4H, s), 1.56 (6H, s). HRMS (M+H) calcd for C<sub>17</sub>H<sub>19</sub>FN<sub>3</sub>O<sub>4</sub>: 348.13597; found: 348.1365. Anal calcd for C<sub>17</sub>H<sub>18</sub>FN<sub>3</sub>O<sub>4</sub>: C, 58.78; H, 5.22; N, 12.09. Found: C, 58.38; H, 5.23; N, 11.80.

**Highlights:**

Synthesis and antiviral activities of series of pyrimidinone carboxamide described

BMS-707035 is a potent HIV-1 integrase strand transfer inhibitor

It displayed good preclinical profiles; advanced to clinical trials

Development halted due to the findings in 12-month dog safety assessment study

ACCEPTED MANUSCRIPT